Supplemental Material: Site-percolation transition of run-and-tumble particles

Soumya K. Saha, Aikya Banerjee, and P. K. Mohanty*
Department of Physical Sciences, Indian Institute of Science Education and Research Kolkata, Mohanpur, 741246 India.

The Supplemental Material provides additional results to support and strengthen the claims of the article. First we discuss the simulation methods and describe the evolution of the RTP system to the steady state. We also provide the finite size scaling collapse for all the critical points, mentioned in the main text.

I. STEADY STATE OF THE MODEL

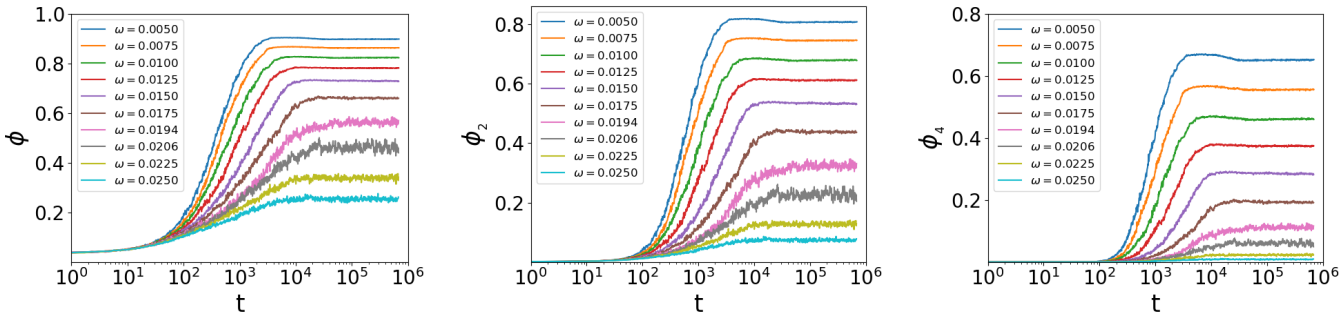

(a) (b) (c)

FIG. 1: Time evolution of (a)ϕ, (b)ϕ_2, and (c)ϕ_4 for $p = 0.235$ and various values of ω, starting from a random initial distribution of $N = L^2/2$ RTPs. Here ϕ_k is the k-th moment of the largest cluster and is given by $\phi_k = \frac{1}{N^k}\langle s_{max}^k \rangle$. Here $L = 128$ and the data is averaged over 200 initial conditions.

From the Monte Carlo simulations of the model defined in Eq. (2) in main text, we calculate the steady state averages of the largest cluster $\phi = \frac{1}{N}\langle s_{max}\rangle$ and the k-th moment, $\phi_k = \frac{1}{N^k}\langle s_{max}^k\rangle$. A cluster is defined in a way similar to the clusters defined in the site percolation problem - two particles separated by one lattice unit belong to same cluster. In Fig. 1 we show for a fixed $p = 0.235$ how ϕ, ϕ_2 and ϕ_4 evolve with time t with different values of ω, starting from a random initial distribution of RTPs on a $L \times L$ square lattice ($L = 128$). The initial orientation of particles are also chosen randomly and independently. It turns out that s_{max} and its moments reach their stationary value well before $t = 10^5$. This gives us an estimate of the relaxation time. In all the simulations we relax the systems until $t = 10^5$ and then calculate the steady state average values in next 10^6 MCS. The steady state data is further averaged over 200 different initial conditions. From these steady state values we obtain the order parameter ϕ, the susceptibility $\chi = \phi_2 - \phi^2$ and the Binder cumulant $U_4 = 1 - \frac{\phi_4}{3\phi_2^2}$.

A. The phase diagram

To obtain the phase diagram we plot the heat map of the order parameter $\langle s_{max}\rangle$ in (ω, p)- plane in Fig. 2(a) where the darker region represent a phase separated state that contains a macroscopic-cluster. The line that separates the mixed phase from the phase-separated state is obtained from a best fit of the the critical points obtained from simulations. Clearly, a re-entrant percolation transition is observed when p is varied keeping ω fixed. With increased p percolated state appears and then then it disappears with further increase of p. Typical largest clusters of the system are shown in Fig. 2(b) at nine different points $(p = 0.02, 0.08, 0.235) \times (\omega = 0.012, 0.022, 0.032)$ marked as circles. The largest cluster is macroscopic (and spans the lattice) for all three values of p when $\omega = 0.012$. Whereas

*Electronic address: pkmohanty@iiserkol.ac.in

for $\omega = 0.022$, the largest cluster is small for $p = 0.08$, it becomes much denser at $p = 0.022$ and becomes sparsely connected again at a larger value of $p = 0.235$ indicating the re-entrant nature of the transition.

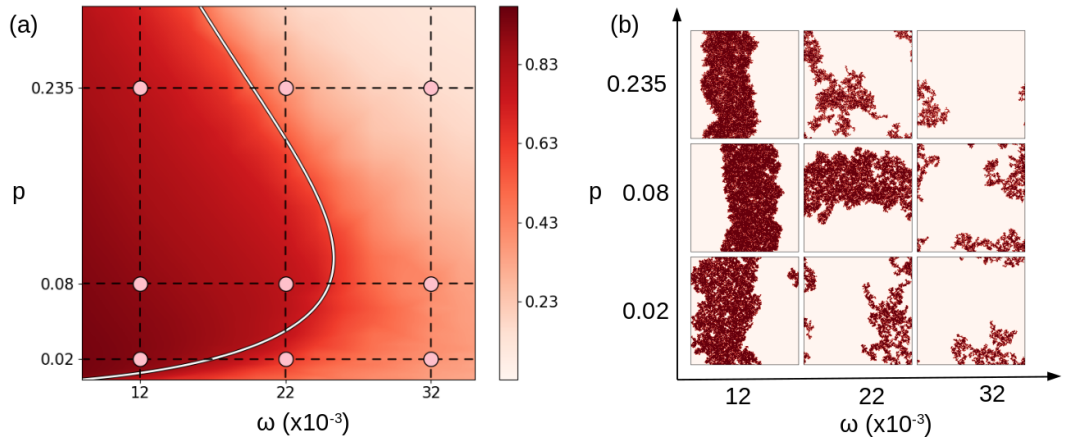

FIG. 2: (a) Phase diagram: The solid line, obtained from the best fit of the critical points, separates the mixed phase from phase separated state. The background is the heat map of the order parameter. (b) Typical largest clusters at nine different points $(p = 0.02, 0.08, 0.235) \times (\omega = 0.012, 0.022, 0.032)$ marked as circles in (a).

B. Critical exponents from finite size scaling

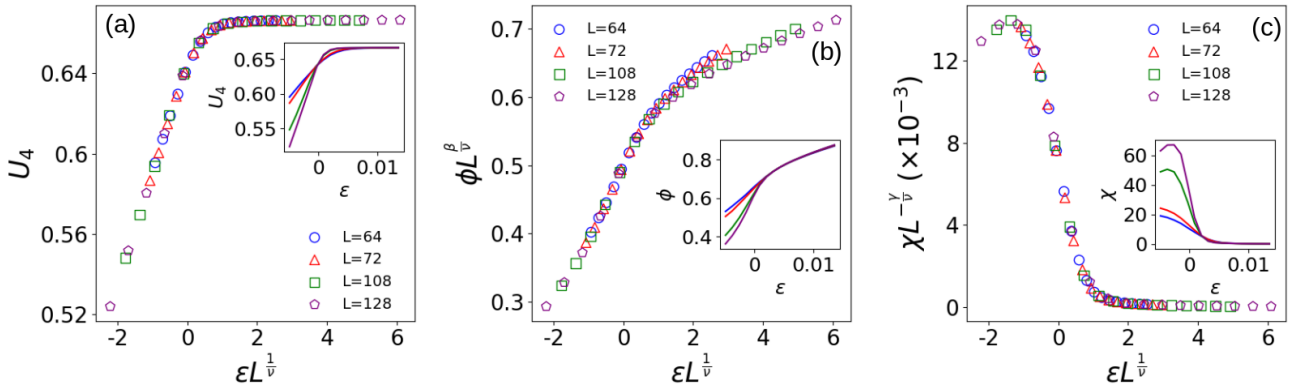

FIG. 3: Critical point II. $(p_c, \omega_c) = (0.150, 0.0235)$: (a)U_4, (b) $\phi L^{\frac{\beta}{\nu}}$ and (c)$\chi L^{-\frac{\gamma}{\nu}}$ as a function of $\varepsilon L^{\frac{1}{\nu}}$. The best collapse is obtained for $\frac{1}{\nu} = 1.26$, $\frac{\beta}{\nu} = 0.10$, $\frac{\gamma}{\nu} = 1.75$. The inset shows raw data, U_4, ϕ, χ vs. ε.

To obtain the static critical exponents ν, β, γ we employ the finite size scaling analysis,

$$\phi = L^{-\frac{\beta}{\nu}} f_\phi(\varepsilon L^{\frac{1}{\nu}});\ \chi = L^{\frac{\gamma}{\nu}} f_\chi(\varepsilon L^{\frac{1}{\nu}});\ U_4 = f_b(\varepsilon L^{\frac{1}{\nu}}). \tag{1}$$

For one of the critical point I. $(p_c, \omega_c) = (0.235, 0.020)$ Figs. 3(a), (b) and (c) in the main text show respectively the scaling collapse of $\phi L^{\frac{\beta}{\nu}}$, $\chi L^{-\frac{\gamma}{\nu}}$ and U_4 as a function of $\varepsilon L^{\frac{1}{\nu}}$. Similar scaling collapse for the other critical points (II to VI mentioned in Table I of the main text) are shown respectively in Figs. 3 to 7.

C. Critical behaviour in p- direction

In a two parameter space there are two independent direction. At any critical point the critical exponents can be obtained from varying one of the paramters keeping the other fixed. So far we have done the finite size scaling analysis

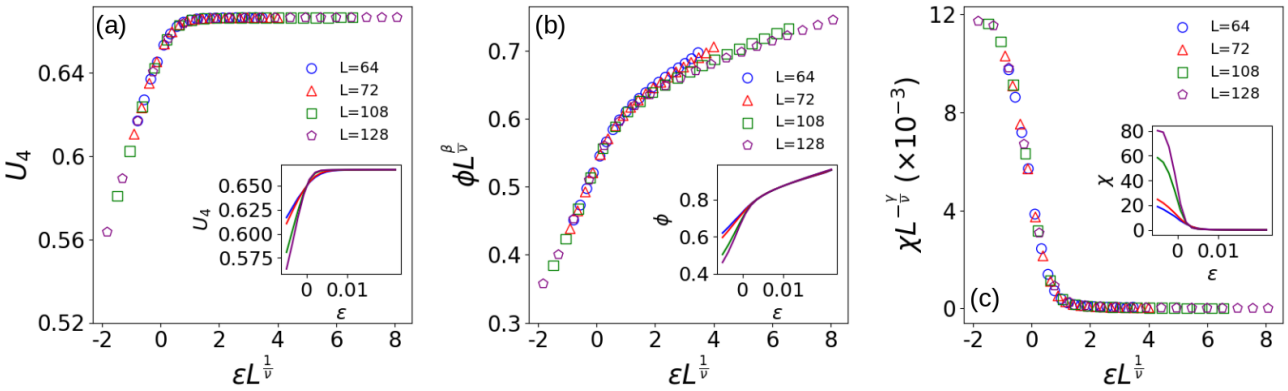

FIG. 4: Critical point III. $(p_c, \omega_c) = (0.080, 0.0247)$: (a)U_4, (b) $\phi L^{\frac{\beta}{\nu}}$ and (c)$\chi L^{-\frac{\gamma}{\nu}}$ as a function of $\varepsilon L^{\frac{1}{\nu}}$. The best collapse is obtained for $\frac{1}{\nu} = 1.22$, $\frac{\beta}{\nu} = 0.09$, $\frac{\gamma}{\nu} = 1.82$. The inset shows raw data, U_4, ϕ, χ vs. ε.

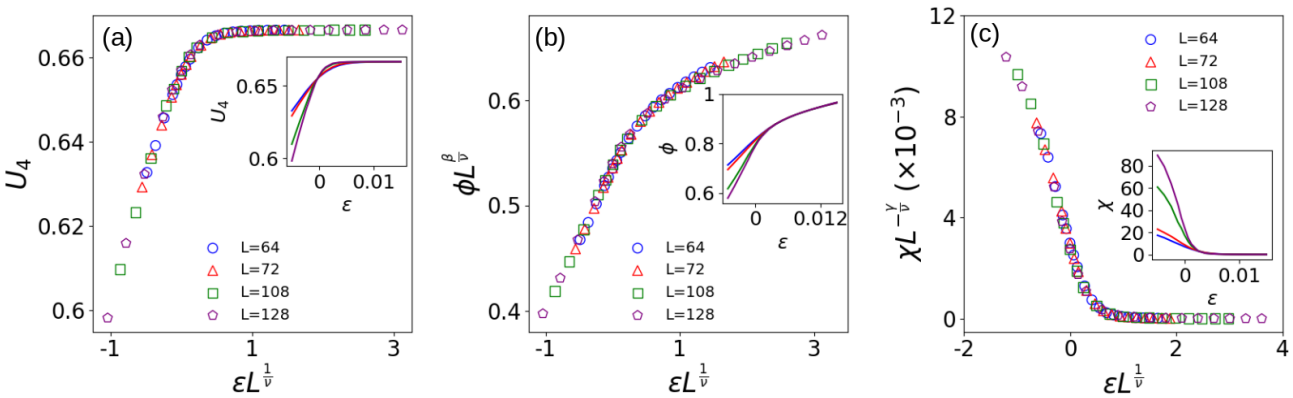

FIG. 5: Critical point IV. $(p_c, \omega_c) = (0.029, 0.020)$: (a)U_4, (b) $\phi L^{\frac{\beta}{\nu}}$ and (c)$\chi L^{-\frac{\gamma}{\nu}}$ as a function of $\varepsilon L^{\frac{1}{\nu}}$. The best collapse is obtained for $\frac{1}{\nu} = 1.13$, $\frac{\beta}{\nu} = 0.066$, $\frac{\gamma}{\nu} = 1.868$. The inset shows raw data, U_4, ϕ, χ vs. ε.

by varying ω for a fixed p. For consistency, we consider one of the critical point $(p_c, \omega_c) = (0.235, 0.020)$, fix $\omega = 0.02$ and study the critical behaviour by varying p. Now the scaling functions depend on $\Delta = p_c - p$,

$$\phi = L^{-\frac{\beta}{\nu}} \tilde{f}_\phi(\Delta L^{\frac{1}{\nu}});\ \chi = L^{\frac{\gamma}{\nu}} \tilde{f}_\chi(\Delta L^{\frac{1}{\nu}});\ U_4 = \tilde{f}_b(\Delta L^{\frac{1}{\nu}}). \tag{2}$$

A plot of $\phi L^{\frac{\beta}{\nu}}$, $\chi L^{-\frac{\gamma}{\nu}}$ and U_4 as a function of $\Delta L^{\frac{1}{\nu}}$ is shown in Fig. 8 where $\frac{\beta}{\nu}$, $\frac{\gamma}{\nu}$ and $\frac{1}{\nu}$ are tuned to a value that gives the best collapse. We find that the critical exponents $\frac{1}{\nu} = 1.43, \frac{\beta}{\nu} = 0.14, \frac{\gamma}{\nu} = 1.72$ obtained previously by varying ε, gives rise to best data collapse.

II. MOTILITY INDUCED PHASE SEPARATION TRANSITION

The RTPs undergo a percolation transition when ω is lowered below a critical threshold value ω_c that depends on p. This percolation transition belong to the super universality class of Z_2 percolation. Should we expect that the motility induced phase separation transition of RTPs also occur occurs at ω_c? In fact, in 2D Ising Model a percolation transition occurs exactly at the same critical temperature T_c where the system phase transit from being a para-magnet to a ferromagnet. The critical behaviour of percolation transition form a new universality class called Z_2-percolation which is different from Ising universality class (IUC). In a similar way, if MIPS occurs in RTP model when ω is lowered below ω_c, what could be a suitable order parameter to characterize such a transition? We use the order parameter suggested in Ref.[3]. It is well-known that in a rectangular system of length L_x and height L_y, the high density phase boundaries align in the shorter direction. Fig. 9(a) shows a typical high density phase (shaded)

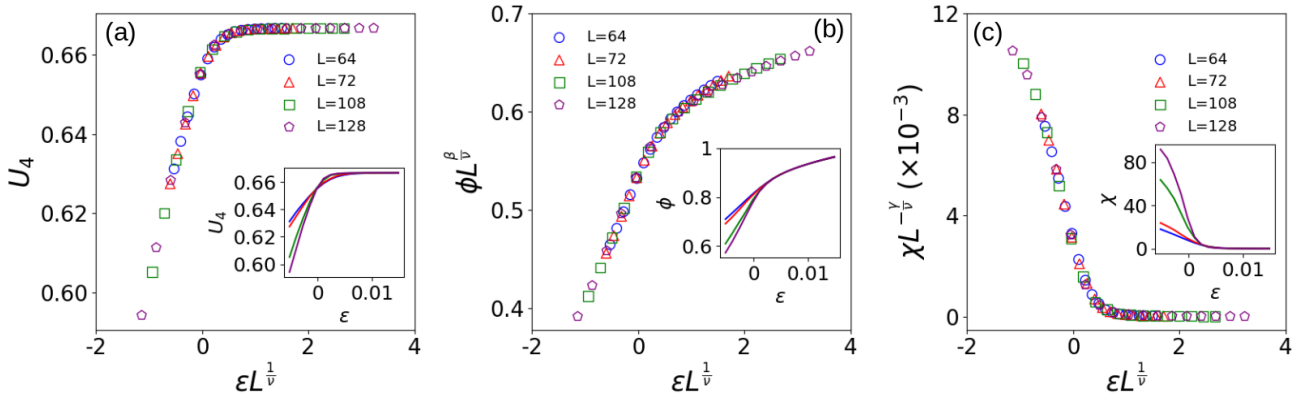

FIG. 6: Critical point V. $(p_c, \omega_c) = (0.0275, 0.019)$: (a)U_4, (b) $\phi L^{\frac{\beta}{\nu}}$ and (c)$\chi L^{-\frac{\gamma}{\nu}}$ as a function of $\varepsilon L^{\frac{1}{\nu}}$. The best collapse is obtained for $\frac{1}{\nu} = 1.11$, $\frac{\beta}{\nu} = 0.065$, $\frac{\gamma}{\nu} = 1.87$. The inset shows raw data, U_4, ϕ, χ vs. ε.

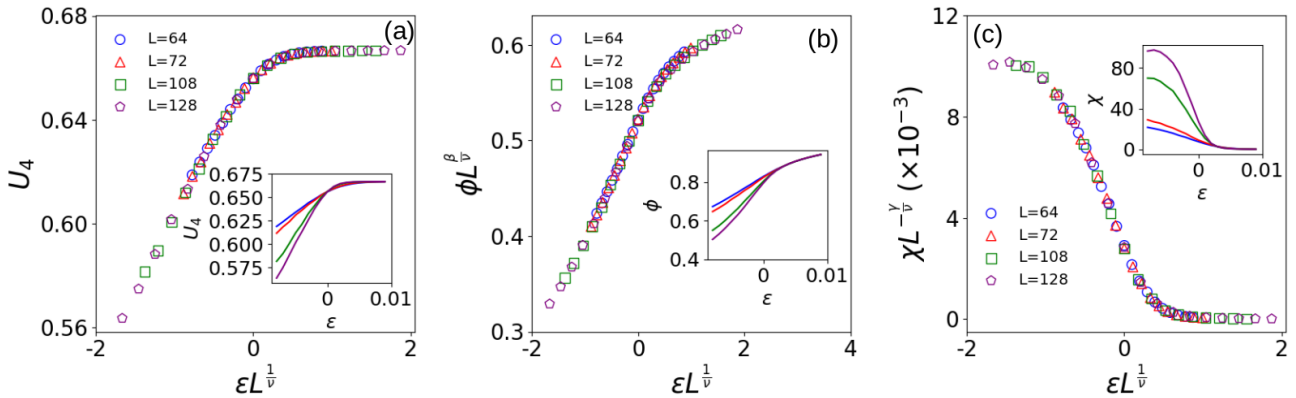

FIG. 7: Critical point VI. $(p_c, \omega_c) = (0.020, 0.018)$: (a)U_4, (b) $\phi L^{\frac{\beta}{\nu}}$ and (c)$\chi L^{-\frac{\gamma}{\nu}}$ as a function of $\varepsilon L^{\frac{1}{\nu}}$. The best collapse is obtained for $\frac{1}{\nu} = 1.10$, $\frac{\beta}{\nu} = 0.055$, $\frac{\gamma}{\nu} = 1.89$. The inset shows raw data, U_4, ϕ, χ vs. ε.

in a system where $L_x = 2L_y$. Then the order parameter ϕ' is defined as [3],

$$\phi' = \frac{2}{L_x L_y} \sum_{x=1}^{L_x} |N_x - \rho L_y| \,; \; N_x = \sum_{y=1}^{L_y} n_{x,y}, \tag{3}$$

where N_x is the total number of particles at lattice sites $\mathbf{i} \equiv (x, y)$ with the same x-coordinate. A schematic representation of how ϕ' quantifies a typical clustered configuration is shown in Fig 9.

Using finite size scaling of the standard order parameter and the corresponding susceptibility at the critical points IV and VI (refer Table 1 of the main text) yields the exponents $\frac{\beta'}{\nu}$ and $\frac{\gamma'}{\nu}$ at those points. The relations between these exponents and the corresponding site-percolation exponents are then verified using Eq. (1) of the main text.

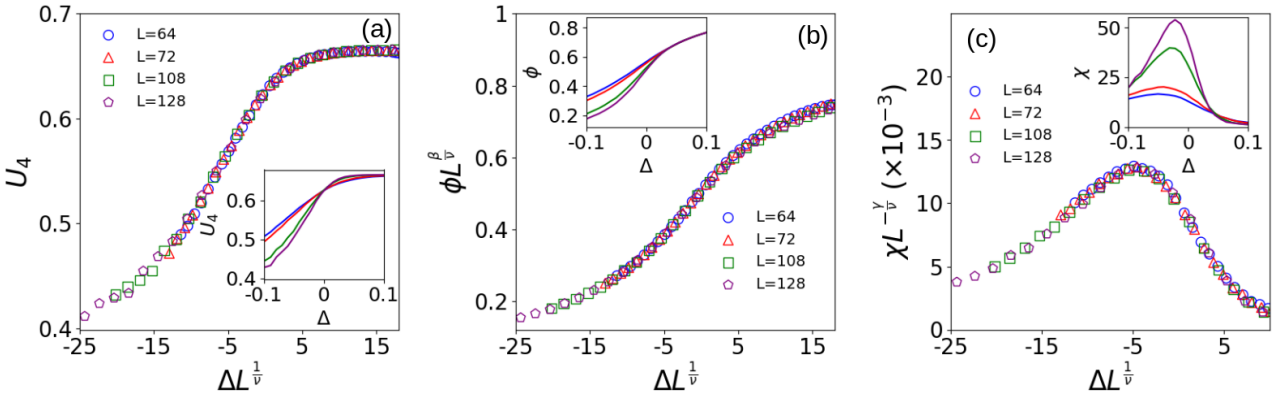

FIG. 8: Critical point IV. $(p_c, \omega_c) = (0.235, 0.020)$: (a)U_4, (b) $\phi L^{\frac{\beta}{\nu}}$ and (c)$\chi L^{-\frac{\gamma}{\nu}}$ as a function of $\Delta L^{\frac{1}{\nu}}$. The best collapse is obtained for $\frac{1}{\nu} = 1.43$, $\frac{\beta}{\nu} = 0.140$, $\frac{\gamma}{\nu} = 1.72$. The inset shows raw data, U_4, ϕ, χ vs. Δ.

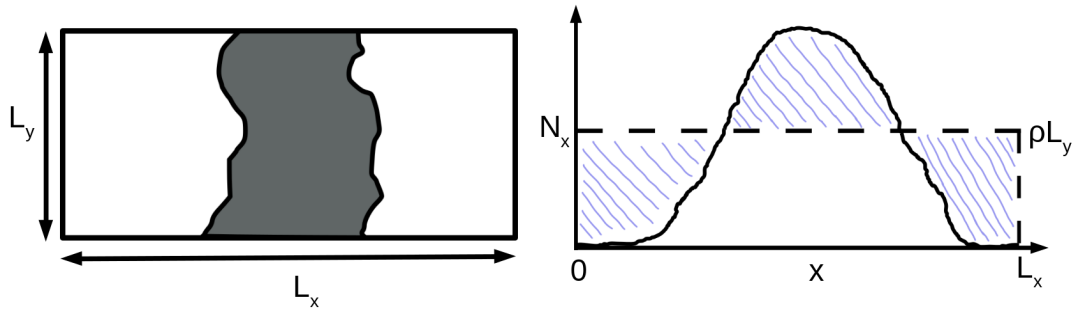

FIG. 9: Schematic configuration of a phase-separated state on a rectangular lattice ($L_x = 2L_y$). (b) The order parameter ϕ' of the system measures how different is N_x from its mean ρL_y in an absolute sense (the shaded area). Here N_x counts the total number of particles at all the lattice sites $\mathbf{i} \equiv (x, y)$ which have same x-coordinate.

[1] K. Binder, D. W. Heermann, *Monte Carlo Simulation in Statistical Physics* (5th Ed.) Springer Berlin, Heidelberg, 2010.
[2] K. Binder, Phys. Rev. Lett. **47**, 693 (1981).
[3] C. G. Ray, I Mukherjee, P. K. Mohanty, J. Stat. Mech.: Theo. and Exp. **2024**, 093207 (2024).